Developmental defects of the ear, cranial nerves and hindbrain resulting from targeted disruption of the mouse homeobox gene *Hox-1.6*

Osamu Chisaka, Teresa S. Musci & Mario R. Capecchi

Howard Hughes Medical Institute, Department of Human Genetics, University of Utah School of Medicine, Salt Lake City, Utah 84112, USA

Gene targeting in mouse embryo-derived stem cells has been used to generate mice with a disruption in the homeobox gene *Hox-1.6*. Mice heterozygous at the *Hox-1.6* locus appear normal, whereas *Hox-1.6*$^-$/*Hox-1.6*$^-$ mice die at or shortly after birth. These homozygotes exhibit profound defects in the formation of the external, middle and inner ears as well as in specific hindbrain nuclei, and in cranial nerves and ganglia. The affected tissues lie within a narrow region along the anteroposterior axis of the mouse but are of diverse embryonic origin. The set of defects associated with the disruption of *Hox-1.6* is distinct from and nonoverlapping with that of the closely linked *Hox-1.5* gene. But both mutations cause loss, rather than homeotic transformation, of tissues and structures.

BY analogy with the genes belonging to the *Drosophila* homeotic complex[1-3], the vertebrate Hox genes are also believed to specify cell identity along the anteroposterior axis of the embryo[4-7]. In man and mouse this family of genes contains 38 members, which are distributed in the genome in four linkage groups, Hox 1-4, on four different chromosomes[8]. To determine the genetic function of some of the Hox genes in the mouse, we have used gene targeting in pluripotent mouse-embryo-derived stem (ES) cells to create mice with specific mutations in these genes[9,10]. Previously it was shown that mice homozygous for a disrupted *Hox-1.5* gene, a member of the Hox 1 linkage group, display developmental defects in several structures derived from a restricted region of the embryo[11]. Here we describe the phenotype of mice homozygous for a targeted mutation in the closely linked gene *Hox-1.6* and discuss the differences between the phenotype we see and that recently described by Lufkin *et al.*[12] in mice homozygous for a targeted mutation in the same gene.

Disruption of *Hox-1.6* in ES cells and mice

Figure 1*a* shows the targeting vector pHox-1.6-N/TK1,TK2 used to disrupt the *Hox-1.6* gene in ES cells. It contains 11.8 kilobases (kb) of mouse genomic sequence encompassing the *Hox-1.6* locus[13,14] with the neomycin-resistance (*neo*^{r}) gene from pMC1neopA[15] inserted into the homeobox domain. Flanking the mouse sequences are the herpes simplex virus thymidine kinase genes TK1 and TK2 (ref. 11). The linearized targeting vector was introduced into ES cells by electroporation, and the cells were then grown in medium containing G418 plus gancyclovir to enrich for transformants that carry the *neo*^{r} gene targeted into one of the endogenous *Hox-1.6* loci[16]. Southern transfer analysis of DNA isolated from G418/gancyclovir resistant colonies showed that 25% of these colonies contained a targeted, disrupted *Hox-1.6* gene. Such an analysis of cell line 1d-5, which contains one copy of the mutated, *neo*^{r}-disrupted *Hox-1.6* allele and one copy of the normal allele is shown in Fig. 1*b*.

Six male chimaeric mice were generated by microinjection of 1d-5 cells into C57Bl/6 recipient blastocysts. Test breeding of the chimaeric males to C57Bl/6 females showed that two of these animals transmitted the ES-derived agouti coat colour to their offspring at a frequency of 100% and 20%, respectively. Mice heterozygous for the *Hox-1.6*$^-$ mutation are fertile and appear normal. The genotypes of littermates derived from intercrosses of *Hox-1.6*$^-$ heterozygotes were evaluated by Southern transfer analyses. Figure 1*d* shows a representative analysis of such a litter. All three expected genotypes are present. The 1:2:1 segregation of *Hox-1.6* alleles among 210 intercross embryos tested, suggests that *Hox-1.6*$^-$/*Hox-1.6*$^-$ embryos are not preferentially aborted or resorbed.

Mice containing two defective copies of the *Hox-1.6* gene die at birth or shortly thereafter, with the longest observed period of survival being 3.5 days. The cause of death has not been determined. But as *Hox-1.6*$^-$/*Hox-1.6*$^-$ mice exhibit hindbrain and cranial nerve defects (see below), physiological functions governed by the hindbrain could be impaired.

Ear compartment defects and distortion of pons

Both inner ear compartments, the middle ear and the external ear are severely affected in *Hox-1.6*$^-$/*Hox-1.6*$^-$ mice. Frontal sections of mutant mice reveal major defects in the formation of the inner ear compartments, the cochlea and the vestibule, the absence of the cochlear and vestibular nerves and the lack of formation of the middle ear ossicles (Fig. 2). In the external ear, the formation of both the auricle and the external acoustic meatus is distorted (Fig. 3).

The homozygous mutant mice also show distortion of the pons (Fig. 2). This appears to result from an accumulation of fluid in the interaural space late in gestation (evident at E19; Fig. 3*d*) and after birth (Fig. 2). This compresses the pons. Two observations argue that the altered pons results from mechanical distortion rather than loss of tissue. First, development of the pons appears normal in earlier stages of gestation (E13.5, E15, E18; data not shown). Second, nuclei of the pons do not appear to be absent, but rather displaced (Figs 2*c*, *d*).

Defects in cranial nerves and ganglia

Figure 4*a* shows an E10.5 control embryo immunoreacted with a monoclonal antibody, 2H3, which labels the 155K neurofilament protein (relative molecular mass 155,000)[17]. The axons associated with the trigeminal (GV), facial (GVII), vestibulocochlear (GVIII), glossopharyngeal (GIX) and vagus (GX) ganglia are clearly discernible. Figure 4*b* and *c* show the 2H3 labelling patterns of two *Hox-1.6*$^-$ homozygous littermates. In both mutant embryos the glossopharyngeal and vagus nerves are poorly developed, and the preganglionic connections with

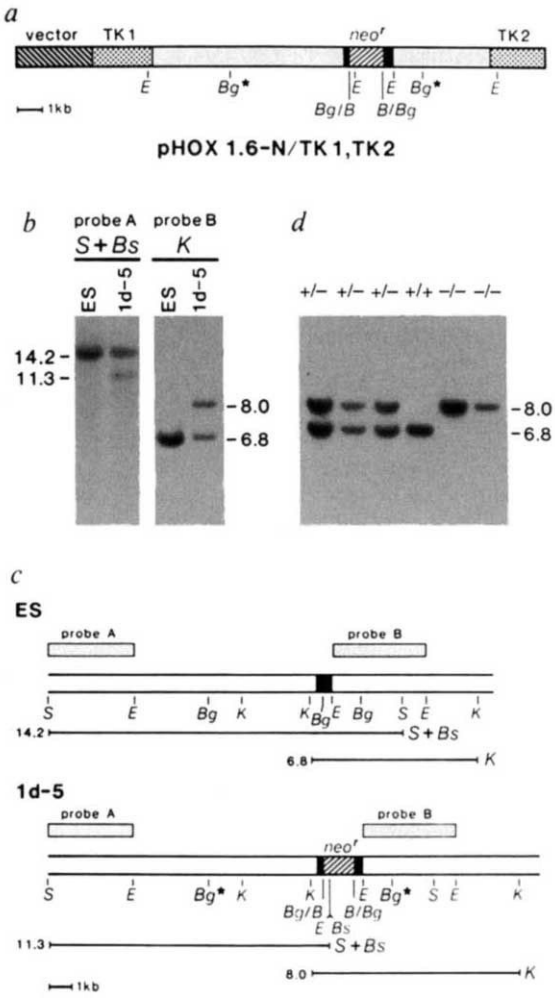

FIG. 1 Southern transfer analysis of ES cell line 1d-5 containing a targeted disruption in the *Hox-1.6* gene (*a*, *b* and *c*) and genotypic analysis of progeny derived from a *Hox-1.6*$^{+}$/*Hox-1.6*$^{-}$ intercross (*d*). *a*, Structure of the targeting vector, pHox-1.6-N/TK1,TK2, used to disrupt the *Hox-1.6* gene in ES cells. Two *Bgl*II sites (indicated as *Bg**) were eliminated by filling in. *b*, Southern blot analysis of DNA from the parental ES cell line CC1.2 and the targeted ES cell line 1d-5. The sizes of the DNA fragments are indicated in kb. DNA samples were digested with *Sca*I (*S*) and *Bst*BI (*Bs*), or *Kpn*I (*K*), electrophoresed through agarose, transferred to nitrocellulose membrane and hybridized with radioactively labelled probe. Probe A (a 3.4-kb *Sca*I–*Eco*RI fragment; see map in *c*) is a 5′ *Hox-1.6* genomic flanking probe, not present in the targeting vector. Probe B (a 3.8-kb *Eco*RI fragment) is a *Hox-1.6* genomic internal probe. In *b*, the reason that the wild-type band (14.2 kb) is more intense than the mutant band (11.3 kb) in 1d-5 DNA is that the ES cells are grown on feeder cells, whose DNA contributes to the signal of the wild-type band. 1d-5 DNA was also analysed using *Bst*XI and *Bgl*II. The *Bgl*II digestion showed that both modified *Bgl*II sites in the targeting vector were transferred to the target locus (data not shown). The *Bst*XI digestion was carried out as a further check to ensure that no other detectable rearrangements of the target locus occurred during the recombination reaction, either 5′ or 3′ to the *neo*^{r} insertion. *c*, Restriction map of the DNA fragments present in the parental and targeted ES cell lines CC1.2 and 1d-5 respectively. *d*, Genotype, as determined by Southern transfer analysis, of 18-day-old embryos from interbreeding of *Hox-1.6*$^{-}$ heterozygous mice. DNA was extracted from tails and analysed. DNA was digested with *Kpn*I and hybridized with internal probe B. The genotype at the *Hox-1.6* locus is indicated above each lane. +/+, Wild type: +/−, heterozygous at *Hox-1.6*; −/−, homozygous for the *Hox-1.6*$^{-}$ allele. *B*, *Bam*HI; *Bg*, *Bgl*II; *Bs*, *Bst*BI; *E*, *Eco*RI; *K*, *Kpn*I; *S*, *Sca*I. The ES cell line CC1.2 was derived from 129/SV/EV mice[30]. The source of blastocysts used to generate chimaeric mice was C57Bl/6J mice. The chimaeric mice were bred to C57Bl/6J mice to test for transmission of the mutant *Hox-1.6*$^{-}$ allele. The resulting *Hox-1.6*$^{-}$ heterozygotes were either interbred or bred to C57Bl/6J mice to maintain the *Hox-1.6*$^{-}$ heterozygous colony and to generate *Hox-1.6*$^{-}$ homozygotes.

the brain stem are not formed. In the mutant embryo shown in Fig. 4*b*, the nerves and VII/VIII ganglia are displaced rostrally towards the trigeminal ganglion. This displacement is even more pronounced for the mutant embryo shown in Fig. 4*c*, resulting in the fusion of GVII/VIII with GV. The nerves associated with GIX and GX also appear to be displaced rostrally along the anteroposterior axis in both embryos. There is a curious asymmetry with respect to the displacement of these nerves/ganglia towards the trigeminal ganglion. It is always more pronounced on the left than on the right side. In six out of six E9.5 and E10.5 embryos that showed the fusion of GVII/VIII with GV, the fusion was observed on the left but not on the right side.

The defects in the cranial nerves depicted in Fig. 4 are also apparent in coronal sections of the same embryos (Fig. 5). For example, the left-side fusion of GVII/VIII with GV is seen in the sections of the *Hox-1.6*$^{-}$ homozygote shown in Fig. 5*e* and *f*. In these embryos, as well as in other E9.5 and E10.5 embryos, the otocyst as well as the ganglia are displaced rostrally towards the trigeminal ganglion (Fig. 5*c*–*f*). Sagittal sections of E9.5 and E10.5 show that the otocyst in the *Hox-1.6*$^{-}$ homozygotes, relative to control embryos, is not only displaced rostrally towards the trigeminal ganglion, but also ventrally towards the pharyngeal arches and away from the neural tube (data not shown). The otocyst in all of the *Hox-1.6*$^{-}$/*Hox-1.6*$^{-}$ embryos examined is smaller and poorly developed. Further, by E11, the endolymphatic duct, which is normally generated as a dorsomedial outgrowth from the otic vesicle, is not formed in the mutant embryos. But the most pronounced feature of these sections is that the characteristic repeating pattern of hindbrain rhombomeres (Fig. 5*a* and *b*) is perturbed in the *Hox-1.6*$^{-}$/*Hox-1.6*$^{-}$ embryos (Fig. 5*c*–*f*). Instead of having the series of bulges

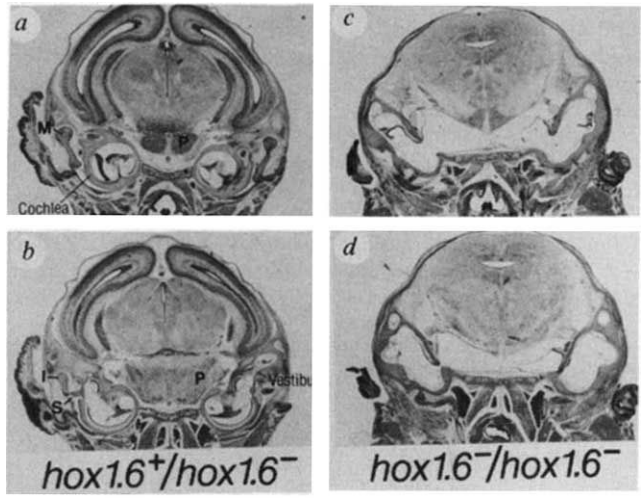

FIG. 2 Comparison of frontal sections (10 microns) prepared from *Hox-1.6*$^{-}$ heterozygous (*a*, *b*) and *Hox-1.6*$^{-}$ homozygous (*c*, *d*) newborn mice. Because the stillborn mutant mice have their heads tilted towards their chest, the angle of the plane of section through the brain is not identical in the control (*a*, *b*) and mutant sections (*c*, *d*). As a result, these sections show tissue from the cerebral hemispheres in the control mouse, but not in the mutant. The sections shown were chosen to illustrate comparable planes in these mice relative to the ears, throat and thorax. The sections from the control mouse (*a*, *b*) illustrate the two inner ear compartments, the cochlea and the vestibule. In the cochlea, the spiral organ of Corti and the cochlear nerve are clearly visible. The vestibule and vestibular nerve are shown in *b*. These sections also show the middle ear ossicles, the malleus (M), the incus (I) and the stapes (S). The corresponding sections from the mutant embryo (*c*, *d*) reveal major defects in the formation of both inner ear compartments, the absence of the cochlear and vestibular nerves within these compartments, and the lack of formation of the middle ear ossicles. In addition, the pons (P) of the *Hox-1.6*$^{-}$ homozygote is highly distorted. Before sectioning, the mice were fixed in Bouin's reagent and embedded in paraffin. Following sectioning, slides were regressively stained with haematoxylin and eosin[31]. The field width of each figure is 7 mm.

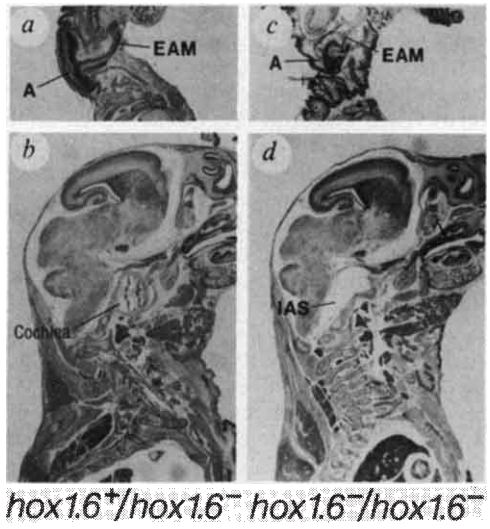

FIG. 3 Comparison of parasagittal sections (10 microns) of E19 *Hox-1.6*$^-$ heterozygote (*a*, *b*) and *Hox-1.6*$^-$ homozygote (*c*, *d*). Sections through the external ear are compared in *a* and *c*. Whereas in the control section a well-formed auricle (A) and external acoustic meatus (EAM) are outlined, these structures are greatly distorted in the *Hox-1.6*$^-$/*Hox-1.6*$^-$ mutant mouse (*c*). In more medial sections of the *Hox-1.6*$^-$ homozygote (*d*), not only is the inner ear absent but the interaural space (IAS) is expanded, distorting the adjacent pons. Note that the forebrain and midbrain of the *Hox-1.6*$^-$ heterozygous and homozygous embryos are indistinguishable. The width of the fields in each figure is 8 mm.

that outline each rhombomere, the walls on both sides of the neural tube of the *Hox-1.6*$^-$ homozygote are smooth. This feature of the hindbrain has been observed in all mutant embryos examined between stages E9.5 and E11.5.

At all stages of embryogenesis and in newborn mice, the trigeminal ganglion and neural structures rostral to the trigeminal ganglion appear normal in *Hox-1.6*$^-$ homozygotes (see examples in Figs 3, 4 and 5). By E13.5, the size of GVII and GVIII in mutant embryos is reduced relative to control embryos, and in a number of mutant embryos the facial ganglion was not detectable. Finally, although the inferior ganglion of the glossopharyngeal and vagus nerves appears fairly normal in E13.5 and E15.5 mutant embryos, the size and shape of the superior ganglia of the same nerves are abnormal. Additionally, the preganglionic connections of the superior ganglia of these nerves with the brain stem and the connections with the inferior ganglia are greatly reduced or absent (data not shown).

Hindbrain defects

At E13.5 through E19, certain hindbrain nuclei are not formed in the mutant embryos. Figure 6*a* and *b* shows transverse sections from E18 control embryos of the hindbrain containing the superior olivary complex (SOC) and facial nuclei (FN) respectively. These hindbrain nuclei are either absent or greatly reduced in comparable sections from the *Hox-1.6*$^-$ homozygous littermates (Fig. 6*c* and *d*).

In the hindbrains of E15, E18, E19 and PO *Hox-1.6*$^-$/*Hox-1.6*$^-$ mice, the dorsal and ventral cochlear nuclei as well as the vestibular nuclei were all seen (data not shown). The possibility of quantitative differences in these nuclei between mutant and control mice needs further analysis. The trigeminal nuclear complex appear normal in the *Hox-1.6*$^-$/*Hox-1.6*$^-$ mice. Also, the ambiguous nuclei associated with the glossopharyngeal and vagus nerves were identified in transverse sections from E18 *Hox-1.6*$^-$ homozygotes and they appear normal.

Discussion

Hox-1.6$^-$ homozygotes exhibit profound defects in the formation of the external, middle and inner ear. These three contiguous, interacting components of the ear are formed by very different embryonic pathways. Development of the inner ear is first evident as a thickening of the surface ectoderm, the otic placode, which then rapidly invaginates to form the otic vesicle (otocyst). Later in development, the vesicle divides into ventral and dorsal components that differentiate into the cochlea and vestibule, respectively. On the other hand, the ossicles of the middle ear are derived from cartilage of the first and second pharyngeal arches, the malleus and incus being primarily derived from first arch cartilage and the stapes from the second[18,19]. Finally, the external auditory meatus develops from a dorsal portion of the first pharyngeal cleft, whereas the auricle develops from six mesenchymal proliferations located at the ends of the first and second pharyngeal arches[18,19]. Despite the difference in embryonic derivation of these components, *Hox-1.6* seems

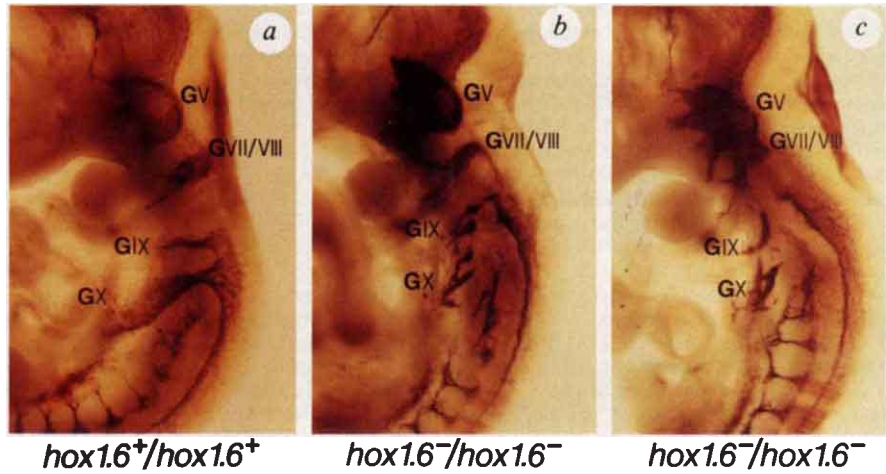

FIG. 4 E10.5 mouse embryos immunoreacted with a monoclonal antibody against the 155K neurofilament protein. *a*, Control *Hox-1.6*$^+$/*Hox-1.6*$^+$ embryo; *b* and *c*, two mutant *Hox-1.6*$^-$/*Hox-1.6*$^-$ embryos. *a*, Control embryo showing axons of the trigeminal ganglion (GV), the facial ganglion (GVII), the vestibulocochlear ganglion (GVIII), the glossopharyngeal ganglion (GIX) and the vagus ganglion (GX). *b* and *c*, Two mutant embryos showing poorly developed glossopharyngeal and vagus nerves and absence of preganglionic connections with the brainstem. Also in the mutant embryos, ganglia GVII through GX appear to be rostrally displaced towards the trigeminal ganglion (GV). The displacement is particularly marked in the *Hox-1.6*$^-$/*Hox-1.6*$^-$ embryo shown in *c*, resulting in the fusion of GVII/GVIII with GV.
METHODS. Embryos were processed according to a protocol from A. Lumsden (personal communication) and fixed in 3.5% formaldehyde/10 mM phosphate buffer (pH 7.4), then washed three times with PBS for 60 min. Endogenous peroxidase activity was blocked by an overnight incubation at 4 °C with 0.05% hydrogen peroxide, 1% Triton X-100, and 1% fetal bovine serum–PBS. Embryos were washed three times with 1% Triton X-100, 1% normal goat serum–PBS (WS) for 60 min and incubated for 4 days at 4 °C with the monoclonal antibody 2H3 (ref. 16) diluted 1:1 with WS; they were then washed three times with WS for 60 min and incubated overnight at 4 °C with goat antimouse-IgG conjugated with horseradish peroxidase (diluted 1:200 with WS). After washing as before, the embryos were incubated with 0.5 mg ml^{-1} diaminobenzidine in 50 mM Tris-HCl, pH 7.4, for 3 h at 4 °C in the dark, followed by a 10-min incubation at room temperature with diaminobenzidine containing 0.018% hydrogen peroxide. The reaction was terminated by three washes with PBS (60 min each). The width of each field shown in *a*–*c* is 2 mm.

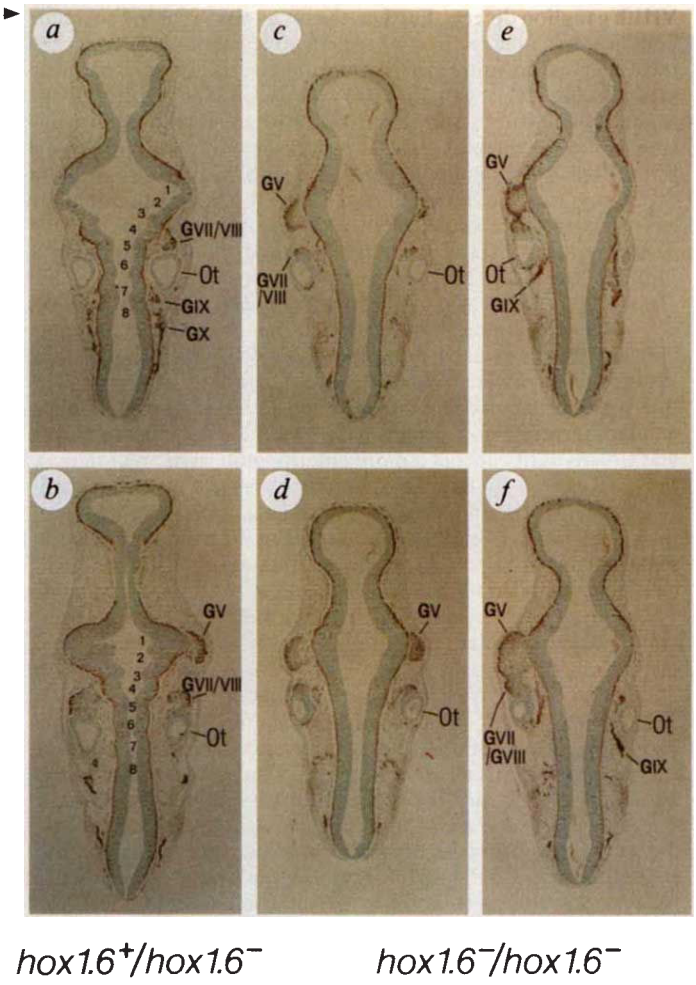

FIG. 5 Comparison of coronal sections (10 microns) of E10.5 embryos immunoreacted with the 155K neurofilament antibody. *a, b*, Control *Hox-1.6*$^{+}$/*Hox-1.6*$^{-}$ embryo; *c–f*, *Hox-1.6*$^{-}$/*Hox-1.6*$^{-}$ mutant embryos. Sections shown in *a, c* and *e* are more dorsorostral than the corresponding sections shown in *b, d* and *f*. These sections were derived from the embryos shown in Fig. 4 and counterstained with methyl green. Note that the rhombomeric pattern of the hindbrain shown in the control embryo (*a, b*) is perturbed in the mutant embryos (*c–f*). Rather than showing the characteristic bulges that outline each rhombomere, the wall on both sides of the neural tube is smooth in the mutant embryos. GIX and GX are poorly developed in the mutant sections. Fusion of GVII/VIII with GV can be seen on the left side of the mutant embryo shown in *e* and *f*. In addition to these ganglia being displaced rostrally towards the trigeminal ganglion, the otocyst (Ot) is also displaced rostrally. The width of each frame is 1.7 mm. The numbers 1–8 in *a* and *b* indicate the approximate positions of rhombomeres 1–8.

to be required for the formation of all of them. *Hox-1.6* could be independently involved in execution of each of these pathways, or there could be a domino effect, with defective *Hox-1.6* regulation of an early component (for example, the inner ear) leading to malformation of a later component, such as the middle ear. Simple versions of the latter hypothesis are, however, contradicted by the existence of many mutations in the mouse and man that can drastically affect the development of the inner ear without affecting development of the middle and external ear[20]. In fact, no previously described mutation in the mouse or man simultaneously affects the formation of inner, middle and external ear. As mentioned, the inner ear is derived from the otocyst. Studies in several species[21] have concluded that development of the membranous labyrinth requires continued passage of inductive signals between the otocyst and the adjacent neural tube. In E9.5 and E10.5 *Hox-1.6*$^{-}$/*Hox-1.6*$^{-}$ embryos, we consistently observed rostral and ventral displacement of the otocyst. Such displacement could interfere with the reception of inductive signals between the otocyst and the neural tube.

Hox-1.6^{-}/*Hox-1.6*$^{-}$ mice also exhibit defects in the hindbrain and associated cranial nerves and ganglia. Particularly prominent is the severe reduction or absence of connections between the glossopharyngeal and vagus nerves/ganglia with the brainstem. This defect is observed as early as E9.5 as a lack of formation of preganglionic connections between these ganglia and the brainstem. Also at E9.5 rostral displacement of GVII through GX towards the trigeminal ganglion is evident, often resulting in the fusion of GVII/VIII with GV. Later in embryogenesis (E13.5 onward), loss of tissue associated with the facial and vestibulocochlear ganglia is observed. This loss could result from either a lack of cell proliferation or atrophy of these tissues. As GVIII is largely of otic placode origin[22], defects affecting the development of this placode could be expected to result in

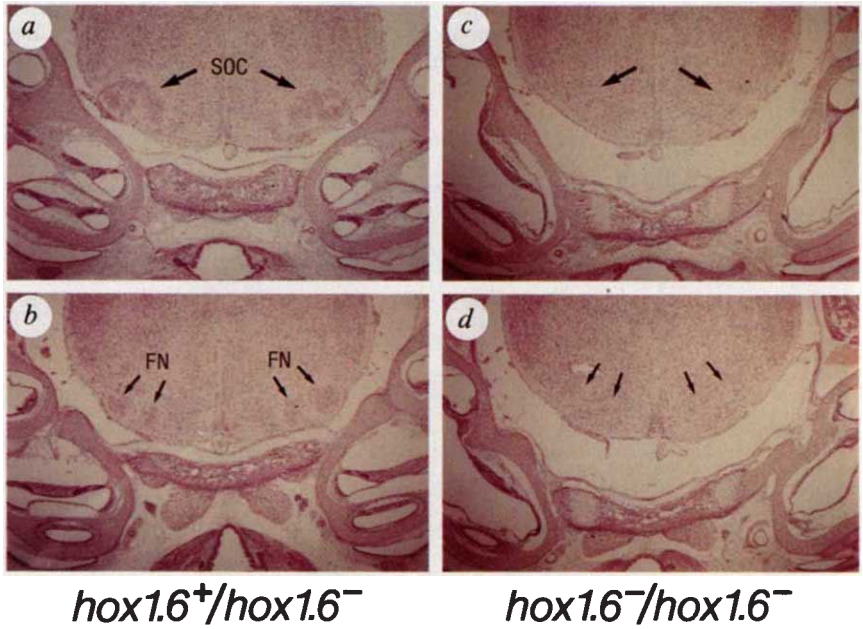

FIG. 6 Comparison of transverse sections (10 microns) of E18 mouse embryos prepared from a control *Hox-1.6*$^{-}$ heterozygote (*a, b*) and a mutant, *Hox-1.6*$^{-}$ homozygote (*c, d*). Sections *b* and *d* are more caudal than those of *a* and *c*. The nuclei of the superior olivary complex (SOC), which are involved in relaying signals from the cochlear nuclei to the inferior colliculus, and the facial nuclei (FN) are shown in the control sections *a* and *b* respectively. These nuclei were not visible in the comparable or adjacent sections from the mutant embryo. At high magnifications a few cells resembling facial motor neurons were seen in the *Hox-1.6*$^{-}$/*Hox-1.6*$^{-}$ section that may represent the remnants of the facial nuclei. Similar patterns were evident in transverse sections from E15 and E19 control and mutant embryos. The width of each field shown in Fig. *a–d* is 3.5 mm.

VIIIth ganglion defects. Further, the target tissue for the cochlear and vestibular nerves is not formed, so it is not surprising that those nerves do not enter their respective inner ear compartments. The facial ganglion (GVII) is derived largely from cephalic neural crest, which arises adjacent to rhombomere 4 (refs 22–26). A phenotypic effect on this neural crest population by the *Hox-1.6*$^-$ mutation is consistent with the reported anterior expression for *Hox-1.6* (refs 12, 27, 28). It is interesting that all neurological defects associated with disruption of *Hox-1.6* are present within a narrow region bounded by rhombomeres 4 through 7 (refs 25, 26).

Careful comparison of *Hox-1.6*$^-$/*Hox-1.6*$^-$ and *Hox-1.5*$^-$/*Hox-1.5*$^-$ mice[11] has revealed no defects in common between the two. Each mutation gives rise to a complex but distinct set of abnormalities. Each set, moreover, is restricted to a limited region along the anteroposterior axis of the mouse embryo, the *Hox-1.6*$^-$ defects being, on the whole, in structures and tissues derived from a more anterior embryonic region than those of *Hox-1.5*$^-$/*Hox-1.5*$^-$. This is consistent with the more anterior limit of expression of the *Hox-1.6* gene. As with *Hox-1.5*, the anterior limit of expression rather than the overall expression pattern, is a better predictor of where mutation of the gene will be expressed phenotypically.

The primordia responsible for the formation of the inner ear, the hindbrain nuclei, the cranial nerves and the associated ganglia affected by disruption of *Hox-1.6* are located in a region of the early embryo encompassing rhombomeres 4–7 (refs 28, 29). The defects in the formation of the middle and external ears may be exceptions. Do these defects represent primary defects in pharyngeal arch-1 and/or associated mesenchymal neural crest? The formation of the auricle requires the intimate interaction between arch-1 and arch-2 mesenchyme, so an arch-2 defect could account for the malformation of this structure. But it is much more difficult to argue that an arch-2 defect could lead to the complete absence of the malleus and the incus because they are derived primarily, if not entirely, from arch-1-associated neural crest[18,19]. Should the lack of formation of these ossicles in the *Hox-1.6*$^-$/*Hox-1.6*$^-$ mice reflect a primary defect in arch-1-associated neural crest, then a paradox exists. Based on experiments that follow migration of neural crest cells in chick embryos, Lumsden *et al.*[29] have proposed that rhombomere 2-associated cephalic neural crest cells migrate into arch 1, rhombomere 4-associated neural crest cells migrate into arch 2, and so on. As the expression pattern of *Hox-1.6* is presumed not to extend into rhombomere 2, we would not anticipate an arch 1-associated phenotype in *Hox-1.6*$^-$/*Hox-1.6*$^-$ mice. There are many ways to reconcile this apparent contradiction. One possibility is that the *neo*^{r} gene inserted into the *Hox-1.6* homeobox is influencing the expression pattern of neighbouring *Hox* genes. If this were the case, that expression does not produce a gain of function phenotype, as *Hox-1.6*$^-$ heterozygotes show no phenotype. Heterozygous mice were examined as carefully as homozygous mice as they were most frequently used as controls. Another possible explanation for the apparent contradiction is that although the majority of rhombomere 4-associated neural crest migrates into the second pharyngeal arch, a subpopulation may migrate into arch 1. A third possibility is that the position of the anterior expression boundary of *Hox-1.6*, particularly during the critical period before the formation of the rhombomere boundaries, has not yet been fully defined. There may be subpopulations of cells that express *Hox-1.6* but are positioned ahead of the visible anterior boundary.

Lufkin *et al.* have also reported on the phenotype of mice containing targeted disruptions in *Hox-1.6* (ref. 12). Their *Hox-1.6*$^-$ phenotype is similar to ours but there are interesting differences. In both cases *Hox-1.6*$^-$/*Hox-1.6*$^-$ mice have defects in the inner ear compartments; however, the extent of the defects appears more extreme in the mice shown in Figs 2, 3 and 6. Lufkin *et al.* did not report that *Hox-1.6*$^-$/*Hox-1.6*$^-$ mice contain middle and external ear defects, whereas we found complete loss of the middle ear ossicles and severe distortion in the formation of the external ear. Similarly, the neuropathology of the respective *Hox-1.6*$^-$/*Hox-1.6*$^-$ mice display similarities and differences. In both cases there was a loss of connections between the brainstem and the glossopharyngeal and vagus nerves. But Lufkin *et al.* did not report the rostral displacement of the cranial ganglia GVII through GX towards the trigeminal ganglion described here. This feature may be more apparent early in embryogenesis than at later stages. Also they did not report the displacement of the otocyst nor the absence of the nuclei of the superior olivary complex. Although we examined eight E9.0–E9.5 embryos, we did not observe a delay in the closure of the neural tube described by Lufkin *et al.* On the other hand, they reported that *Hox-1.6*$^-$ homozygotes have normal rhombomere morphology, whereas we consistently observe that between E9.0–E11.0 the rhombomeres in the mutant hindbrain do not exhibit the characteristic bulges that outline each rhombomere. The reported defects in the basioccipital bone, as well as in the bones and cartilages associated with the inner ear, are similar in the two mutant mice (data not shown).

Some of the differences in the phenotype could arise from the differences in the mutant alleles of *Hox-1.6* created by the two groups. Two transcripts are generated from the *Hox-1.6* locus as a result of alternative splice sites within the *Hox-1.6* gene[13,14,28]. One transcript directs the synthesis of the entire *Hox-1.6* protein product, including the homeobox domain. The second transcript may direct the synthesis of a truncated protein with the same NH_2^- terminus but lacking the homeobox domain. The *Hox-1.6*$^-$ mutant allele made by Lufkin *et al.*[12] is predicted to eliminate the synthesis of both transcripts, whereas our mutant allele should disrupt the synthesis of only the intact homeobox-containing protein. □

Received 16 September; accepted 30 December 1991.

1. Akam, M. *Development* **101,** 1–22 (1987).
2. Gehring, W. J. *Science* **236,** 1245–1252 (1987).
3. Ingham, P. N. *Nature* **335,** 25–34 (1989).
4. Holland, P. W. H. & Hogan, B. L. *Genes Dev.* **2,** 773–782 (1988).
5. Duboule, D. & Dollé, P. *EMBO J.* **8,** 1497–1505 (1989).
6. Graham, A., Papalopulu, N. & Krumlauf, R. *Cell* **57,** 367–378 (1989).
7. Kessel, M. & Gruss, P. *Science* **249,** 374–379 (1990).
8. Acampora, D. *et al. Nucleic Acids Res.* **17,** 10385–10401 (1989).
9. Capecchi, M. R. *Trends Genet.* **5,** 70–76 (1989).
10. Capecchi, M. R. *Science* **244,** 1288–1292 (1989).
11. Chisaka, O. & Capecchi, M. R. *Nature* **350,** 473–479 (1991).
12. Lufkin, T., Dierich, A., LeMeur, M., Mark, M. & Chambon, P. *Cell* **66,** 1105–1119 (1991).
13. Baron, A. *et al. EMBO M.* **6,** 2977–2986 (1987).
14. LaRosa, G. J. & Gudas, L. J. *Molec. cell. Biol.* **8,** 3906–3917 (1988).
15. Thomas, K. R. & Capecchi, M. R. *Cell* **51,** 503–512 (1987).
16. Mansour, S. L., Thomas, K. R. & Capecchi, M. R. *Nature* **336,** 348–352 (1988).
17. Dodd, J., Morton, S. B., Karagogeos, D., Yamamoto, M. & Jessel, T. M. *Neuron* **1,** 105–116 (1988).
18. Noden, D. M. & Van de Water, T. R. in *The Biology of Change in Otolaryngology* (ed. Ruben, R. J., Van de Water, T. R. & Rubel, E. W.) 15–46 (Elsevier, New York, 1986).
19. Van de Water, T. R., Maderson, P. F. A. & Jaskoll, T. F. in *Morphogenesis and Malformation of the Ear* (ed. Gorlin, A. R.) 147–180 (Liss, New York, 1980).
20. Deol, M. S. in *Morphogenesis and Malformation of the Ear* (ed. Gorlin, A. R.) 243–261 (Liss, New York, 1980).
21. Van de Water, T. R., Cheak, W. L., Ruben, R. J. & Shea, C. A. in *Morphogenesis and Malformation of the Ear* (ed. Gorlin, A. R.) 5–45 (Liss, New York, 1980).
22. Altman, J. & Bayer, S. in *Advances in Anatomy, Embryology and Cell Biology* **74,** 1–90 (Springer, New York, 1982).
23. Le Douarin, N. in *The Neural Crest* (Cambridge Univ. Press. UK, 1983).
24. Noden, D. M. *Development* **103** (suppl.), 121–140 (1988).
25. Lumsden, A. & Keynes, R. *Nature* **337,** 424–428 (1989).
26. Hunt, P., Wilkinson, D. & Krumlauf, R. *Development* **112,** 43–50 (1991).
27. Sundin, O. H. *et al. Development* **108,** 47–58 (1990).
28. Murphy, P. & Hill, R. E. *Development* **111,** 61–74 (1991).
29. Lumsden, A., Sprawson, N. & Graham, A. *Development* (in the press).
30. Bradley, A., Evans, M., Kaufman, M. H. & Robertson, E. *Nature* **309,** 255–256 (1984).
31. Thomas, K. R. & Capecchi, M. R. *Nature* **346,** 847–850 (1990).

ACKNOWLEDGEMENTS. We thank M. Allen, D. Harris, C. Lenz, E. Nakashima and S. Tamowski for technical assistance, J. Conlee and H. Yip for advice on the neuroanatomy, and J. Dodd for the monoclonal antibody 2H3.